

An investigation of nuclear collisions with a momentum-dependent Lattice Hamiltonian model.

D. PERSRAM and C. GALE

*Department of Physics, McGill University, 3600 University Street
Montréal, Québec H3A 2T8, Canada*

Abstract. We formulate a Lattice Hamiltonian approach for the modeling of intermediate energy heavy ion collisions. After verifying stationary ground state solutions, we implement this in a calculation of nuclear stopping power and compare our results with experimental data. Our findings support a relatively soft nuclear equation of state, with a momentum-dependent self-consistent mean field.

INTRODUCTION

For the past two decades the field of heavy ion collisions has seen many advances on both the experimental and theoretical fronts. At low and intermediate energies, much progress has come from the solution of transport theories such as the BUU [1–3] and QMD [4,5] models. Both have been quite successful in explaining many observables extracted from experimental studies at energies ranging from a few hundred MeV per nucleon up to a few GeV per nucleon. In this work, we concentrate on the first approach. Precise measurements in the lower energy regime ($\sim \epsilon_f$) have specified the need for precise numerical models. Previous BUU solutions have employed the so called “test particle” method [3]. However, it has been shown that at low energies this method may lead to solutions that can badly violate energy conservation [6]. This aspect is expected to worsen as the bombarding energy is decreased. The energy conservation problem inherent in the test particle method has largely been circumvented through the “Lattice Hamiltonian” [7] algorithm.

The process of colliding ions involves a mixture of interactions that the individual nucleons themselves undergo. For collisions above ϵ_f , nucleons can interact with each other via elastic and inelastic scattering. For the latter process to occur, the energy available in the nucleon-nucleon centre of mass frame must be at least $E = 2m_n + m_\pi$ since the lightest meson is the π meson. In addition to hard scattering, the nucleons also experience a self-consistent nuclear mean field. Thus, the nucleons will move on curved trajectories.

The mean field is a crucial ingredient in any transport calculation. Various *nuclear* mean fields have extensively been studied in the past [8–10]. In addition, it has previously been shown that different parameterizations of the nuclear mean field can yield similar results in measurements of transverse flow as can be seen in reference [8,9]. However transverse flow measurements do not exhaust the presently available experimental observations. In fact there are now available experimental data which can serve to distinguish between different parameterizations. This is the subject of this work.

NUCLEAR MATTER POTENTIALS

We begin our discussion by starting with nuclear matter considerations. The latter is defined as a net isospin zero infinite system of nucleons in which the total electric charge of the system is zero. Thus, isospin and Coulomb effects are not considered. We will use a semi-classical approximation which allows us to simultaneously specify the positions and momenta of all nucleons at all times. If we assume a smooth phase space distribution function $f(\vec{r}, \vec{p})$, the total energy of the system reads:

$$\begin{aligned}
 E &= T + U \\
 &= \int d^3r d^3p f(\vec{r}, \vec{p}) \frac{p^2}{2m} \\
 &\quad + \frac{1}{2} \int d^3(r, r', p, p') f(\vec{r}, \vec{p}) f(\vec{r}', \vec{p}') v^{(2)}(\vec{r}, \vec{r}', \vec{p}, \vec{p}') + \frac{1}{3!} \int \dots
 \end{aligned} \tag{1}$$

In equation 1, $v^{(2)}(\dots)$ represents a two-body nucleon-nucleon interaction. The potential energy term is written as a sum of n body interactions. Thus, our potential in general contains both two-body as well as many-body interactions. Next, we need to adopt a specific form for our n body interaction terms. A first simple choice is a momentum-independent contact interaction of strength a , and for the two-body direct term reads:

$$v^{(2)}(\vec{r}, \vec{r}', \vec{p}, \vec{p}') = a\delta(\vec{r} - \vec{r}'). \tag{2}$$

If we lump the 3-body and higher interaction potentials into one term, we arrive at the “generalized Skyrme interaction” [11]. The corresponding potential energy *density* is shown below. The three parameters A , B and σ are left for us to choose, on the condition that we respect some constraints. We will discuss these in the next section.

$$W(\vec{r}) = \frac{A}{2} \frac{\rho^2(\vec{r})}{\rho_0} + \frac{B}{\sigma + 1} \frac{\rho^{\sigma+1}(\vec{r})}{\rho_0} \tag{3}$$

This generalized Skyrme interaction has been extensively studied in the context of heavy-ion collisions and has shown some success in describing a large amount

of heavy-ion collision data at intermediate energies ($\sim 1\text{GeV}/A$) with transport-type models [3,9,12,13]. However, there are other properties of nuclear matter that will manifest themselves during heavy-ion collisions which have yet to be unveiled. It is well known that the nuclear optical potential is strongly momentum-dependent [14–16]. The simple phenomenological potential above does not contain any momentum-dependence. Thus, in order to obtain a more realistic description of nuclear matter one should include a term in the potential which includes some functional dependence on momentum. In this work, we use the Fourier transform of the finite range Yukawa potential. This momentum dependent interaction is then coupled with the zero range momentum-independent interaction and yields the following nuclear matter potential energy density shown below. This potential is known as the “MDYI” potential [17].

$$W(\vec{r}) = \frac{A}{2} \frac{\rho^2(\vec{r})}{\rho_0} + \frac{B}{\sigma + 1} \frac{\rho^{\sigma+1}(\vec{r})}{\rho_0} + \frac{C\Lambda^2}{\rho_0} \int \int d^3p d^3p' \frac{f(\vec{r}, \vec{p})f(\vec{r}, \vec{p}')}{\Lambda^2 + (\vec{p} - \vec{p}')^2} \quad (4)$$

Skyrme and MDYI parameters

In the last section, two parameterizations of the nuclear mean field potential for nuclear matter were given. In both of those parameterizations, a number of “free” parameters were left unspecified. There are three for the Skyrme interaction and two additional ones (for a total of five) for the MDYI interaction. In order for these potentials to give a physical representation of nuclear matter, the value of each of the parameters must some how be connected to properties of nuclear matter. We use the experimentally observed properties of heavy ions to fix these parameters.

Let us first consider the momentum-independent Skyrme interaction. Two obvious conditions that should be satisfied are the binding energy per nucleon ($E_B = 16$ MeV) and the equilibrium density for nuclear matter ($\rho_0 = 0.16 \text{ fm}^{-3}$). Both of these are well established quantities [18]. A third condition that one can use to fix the three parameters is the determination of the nuclear matter compressibility (K). This quantity is directly related to the equation of state and gives a measure of the scalar elasticity of nuclear matter. For example, a soft or low value of the compressibility results in matter which is easily deformed by an external force while a stiff or high value provides matter which is relatively impervious to deformations. The value of the nuclear matter compressibility can be taken from the giant monopole resonance or breathing mode observed in heavy ions [19]. In addition, supernova calculations can provide additional constraints on this value [20]. The goal of this work is to attempt to deduce a value of the nuclear mean field compressibility from simulations of colliding heavy ions. We have chosen to use two values for the compressibility; a relatively soft EOS is provided with the choice of $K = 200$ MeV and a stiff EOS is provided with $K = 380$ MeV. These two values provide a reasonable bracket on this quantity as can be seen from supernova calculations as well as breathing mode calculations and observations [19–21].

The momentum-dependent MDYI interaction used in this work requires that we specify two more parameters. In equation 4, C represents the strength of the momentum-dependent term and Λ is representative of a range in momentum space. We now turn to nucleon-nucleus scattering experiments wherein one can extract information on the nuclear optical potential. This quantity is directly related to equation 4 as the latter contains information about the nucleon single particle potential ($U(\rho, \vec{p})$) inside nuclear matter. By requiring $U(\rho = \rho_0, \vec{p} = 0) = -75$ MeV and $U(\rho = \rho_0, \vec{p}^2/2m = 300 \text{ MeV}) = 0$ we provide the two extra conditions necessary to fix all five parameters in the MDYI interaction potential. The agreement obtained with experimental measurements is very good from kinetic energies ranging from zero up to the GeV per nucleon regime [22]. With these parameterizations, we are now in a position to apply our nuclear transport model to the simulation of heavy ions collisions.

SIMULATION OF HEAVY IONS/COLLISIONS

In order to simulate colliding nuclei, there are still a few ingredients that we must add to the above nuclear matter approach. First, any stable nucleus contains a non-zero number of protons and is thus charged. We expect the Coulomb potential to play a role. Secondly, many heavy nuclei have a neutron number which can be as high as 1.5 times the atomic number: total isospin is non-zero. It is therefore also necessary to include an isospin potential into our formalism. We use an isospin potential that has previously been used in astrophysical considerations [23]. Now the total Hamiltonian of an A nucleon nucleus can be written down. The potential energy is discretized on a lattice(δx) in configuration space. We show below this Hamiltonian where α is a configuration space grid index.

$$H = \sum_{i=1}^A \frac{p_i^2}{2m} + (\delta x)^3 \sum_{\alpha} (W_{\alpha} + W_{\alpha}^{coul} + W_{\alpha}^{iso}) \quad (5)$$

In the above, W_{α} can either be the Skyrme or MDYI potential energy density.

As our Hamiltonian in equation 5 has no explicit time dependence, energy is conserved and we can now calculate the binding energy per nucleon for any size nucleus. We performed such a calculation for ~ 30 nuclei ranging from mass number $A: 4 \rightarrow 260$ for both the Skyrme and MDYI potential energy densities. We obtain very good agreement with the Weizacker semi-empirical mass formula [18] over a large mass range. In passing, we note that the absence of an *explicit* surface potential yields about 1 MeV/A too large a binding energy for light nuclei. We do not expect this to significantly alter the results of this work.

The above analysis was done for a stationary nucleus. However, in heavy ion collision physics, one is concerned with the interaction of nuclei. Thus, we would like to know how the nucleons that make up two colliding nuclei evolve in time. We want to study the dynamical, *non-equilibrium* behaviour of colliding nuclei. In other words, we would like to have the equations of motions for all nucleons in this

scenario. Obtaining this is a simple matter since we have the total Hamiltonian of the system. Thus, one has Hamilton's equations.

$$\dot{\vec{r}}_i = \nabla_{\vec{p}_i} H \qquad \dot{\vec{p}}_i = -\nabla_{\vec{r}_i} H \qquad (6)$$

The coupled set of nonlinear equations 6 together with equation 5 represent the *Lattice Hamiltonian* solution for colliding nuclei [7].

So far, we are able to calculate the trajectories of all nucleons in a time varying self-consistent mean field. However, as mentioned in the introduction one must also allow for elastic and inelastic nucleon-nucleon collisions as the total nucleon-nucleon cross section is in general non-zero. For the application of the model we have developed so far we will only be concerned with energies below the particle production threshold thus we need only consider the elastic nucleon-nucleon cross section. As we have included an isospin potential in our formulation, we will be using an elastic scattering cross section that is parameterized in terms of isospin and centre of mass energy [24]. For a detailed prescription of the scattering procedure used in this work the reader is referred to the reference by Bertsch and Das Gupta [3]. The details for solving Hamilton's equations in our model can be found in reference [25].

Now we are in a position to test the predictive power of the model. This is the subject of the following section.

NUCLEAR STOPPING

In order to give a qualitative picture of nuclear stopping it is instructive to consider two extreme examples of colliding nuclei. One can envisage that as two heavy ions approach each other on a collision course, there is a possibility for the two nuclei to coalesce. As two nuclei approach they are slightly slowed down by the Coulomb barrier. If the incident energy is just above that of the Coulomb barrier, the nuclei can merge into one large "nucleus". If the initial energy is sufficiently low such that there is no large buildup of density, repulsive mean field forces are at a minimum and a large compound nucleus will remain (assuming the Coulomb forces are not large enough to fission the nucleus). On the other hand, if one considers a high energy collision, there are regions where the matter density builds up rapidly and creates domains of large (positive) energy density. This in turn produces large pressure gradients which tend to expel the nucleons, thus breaking up the transient system. In the end we are left with many small remnants. At energies between these two extremes, experiments tell us that the final state can consist of a relatively large remnant with many smaller remnants in the final state. In order to quantify the stopping power and to compare with a specific experimental measurement, we will consider only the largest of these remnants. If we move to the lab frame, in the case of a single remnant, the latter will have a velocity equal to the velocity of the centre of mass of the two nuclei. At higher energies when there are more than one remnant present the velocity of the heaviest remnant will

be smaller than in the previous case. This is due to the many small remnants which carry away a portion of the initial momentum. Thus, for a large final state remnant velocity, we have large stopping or close to complete absorption of the projectile. For a small final state remnant velocity, there is little stopping of the projectile as it partially rifles through the target. This description is exactly what is termed “nuclear stopping”. Our goal here is to quantitatively investigate what role the nuclear matter compressibility as well as the momentum-dependence of the nuclear mean field play in determining the stopping power of nuclei.

Simulation results

Recent nuclear stopping results have been obtained at the NSCL at MSU using the K1200 cyclotron [26]. The longitudinal lab frame velocity of the heaviest remnant was determined for $^{40}\text{Ar}+^{108}\text{Ag}$. The laboratory beam energies studied there ranged from $\sim 8 \rightarrow 115$ MeV/A. The experimental impact parameters were estimated from charged particle multiplicity and for the Ar+Ag system corresponds to $b \sim b_{max}/4$ [27]. In an attempt to bracket the experimental data we have performed Lattice Hamiltonian simulations for the Ar+Ag system at $b = b_{max}/3$ and $b = b_{max}/5$ for bombarding energies ranging from $\sim 20 \rightarrow 120$ MeV/A. The calculations were performed with both the Skyrme and MDYI nuclear mean field potentials as well

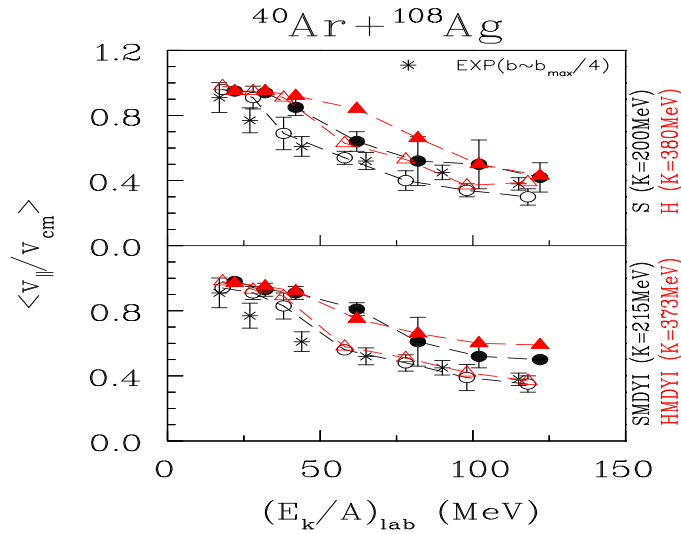


FIGURE 1. Fractional longitudinal laboratory frame velocity of the heaviest post-collision remnant as a function of laboratory bombarding energy. The experimental measurements [26] are shown by asterisks and the Lattice Hamiltonian calculations are shown with open and solid symbols. The circles are for a soft EOS and the triangles are for a stiff EOS. The filled(open) symbols are for an impact parameter of $b = b_{max}/5(b = b_{max}/3)$. The top panel is with a Skyrme interaction and the bottom panel is with the MDYI interaction.

as with a stiff and soft EOS. For the Skyrme(MDYI) interaction, the compressibilities were 200(215)MeV for the soft EOS and 380(373)MeV for the stiff EOS. These parameterizations have been used before in a work by Zhang, Das Gupta and Gale [28].

Figure 1 displays the result for the longitudinal lab frame velocity of the heaviest remnant for both the measurement and calculation. Several conclusions can be taken from this. First, we note that the momentum-dependent mean field result is less sensitive to the value of the nuclear matter compressibility than is the momentum-independent mean field result. Indeed, the MDYI potential shows little sensitivity to the compressibility for this observable. This decrease in sensitivity is not too surprising once one takes into account the fact that the momentum-independent mean field is driven by the nuclear compressibility only while the momentum-dependent mean field contains an additional dependence on the momentum distribution. We find that the most convincing result for the momentum-independent mean field is obtained with a soft EOS. Both EOS's for the momentum-dependent mean field show nice agreement with the data for the larger value of the impact parameter.

Another observable considered was the mass of the heaviest remnant. These results are shown in figure 2. Note that from these results we can now separate the two momentum-dependent mean fields. As far as the momentum-dependent mean field is concerned (bottom panel), we find better agreement with a soft EOS. The data are only slightly underestimated in this case and the trend is reproduced. The momentum-independent mean field result on the other hand favours a stiff EOS. This is in contrast to the stopping result and indicates that one cannot satisfy both observables with the same momentum-independent mean field.

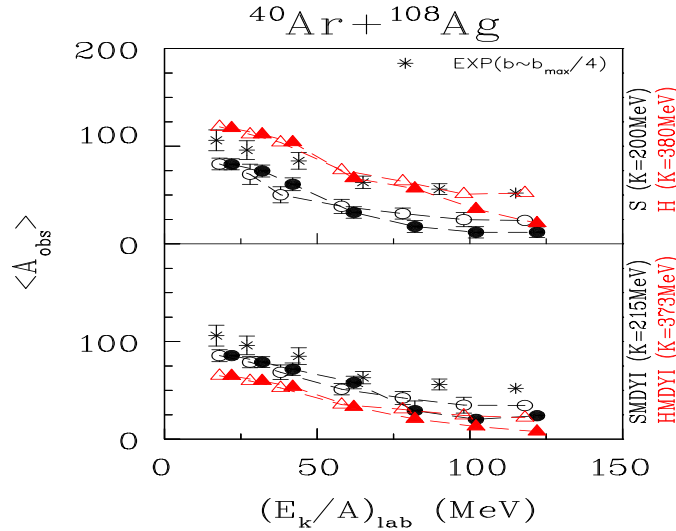


FIGURE 2. Observed mass of the heaviest remnant. All symbols and panels are as in figure 1.

CONCLUSION

We have implemented a Lattice Hamiltonian simulation for the case of two colliding heavy ions. Our solution incorporates both a momentum-independent as well as momentum-dependent nuclear mean field. The nuclear stopping results indicate that the momentum-dependent mean field is less sensitive to the nuclear matter compressibility than is the momentum-independent mean field. Furthermore, satisfactory agreement with both the stopping data and the observed large remnant mass can be achieved with the use of a momentum-dependent nuclear mean field. Our results support a relatively soft EOS of compressibility $K = 215\text{MeV}$.

REFERENCES

1. E. A. Uehling and G. E. Uhlenbeck, *Phys. Rev.* **43**, 552 (1933).
2. G. F. Bertsch, H. Kruse and S. Das Gupta, *Phys. Rev.* **C29**, 673 (1984).
3. G. F. Bertsch and S. Das Gupta, *Phys. Rep.* **160**, 189 (1988).
4. J. Aichelin and H. Stöcker, *Phys. Lett.* **B176**, 14 (1986).
5. J. Aichelin, *Phys. Rep.* **202**, 233 (1991).
6. C. Gale and S. Das Gupta, *Phys. Rev.* **C42**, 1577 (1990).
7. R. J. Lenk and V. R. Pandharipande, *Phys. Rev.* **C39**, 2242 (1989).
8. C. Gale, G.M. Welke, M. Prakash, S.J. Lee and S. Das Gupta, *Phys. Rev.* **C41**, 1416 (1990).
9. Qiubao Pan and Pawel Danielewicz, *Phys. Rev. Lett.* **70**, 2062 (1993).
10. G.F. Bertsch, W.G. Lynch and M.B. Tsang, *Phys. Lett.* **B189**, 384 (1987).
11. T.H.R. Skyrme, *Nucl. Phys.* **9**, 615 (1959).
12. G.D. Westfall et. al., *Phys. Rev. Lett.* **71**, 1986 (1993)
13. M.B. Tsang et. al., *Phys. Rev.* **C53**, 1959 (1996).
14. B. Friedman and V.R. Pandharipande, *Phys. Lett.* **B100**, 205 (1981).
15. J.P. Jeukeune, A. Lejeune and C. Mahaux, *Phys. Rep.* **25C**, 83 (1976).
16. R. Maffiet, *Prog. Part. Nucl. Phys* **21**, 207 (1988).
17. C. Gale et. al., *Phys. Rev.* **C41**, 1545 (1990).
18. See, for example, Samuel S.M. Wong *Introductory Nuclear Physics*, Prentice-Hall, Inc. Englewood Cliffs, New Jersey (1990).
19. D. H. Youngblood, H.L. Clark and Y.W. Lui, *Phys. Rev. Lett.* **82**, 691 (1999).
20. See, for example, H.A. Bethe, *Rev. Mod. Phys.* **62**, 801 (1990), and references therein.
21. M.M. Sharma, **nucl-th/9904036**, D. Vretenar et. al., **nucl-th/9612042**.
22. László P. Csernai, George Fai, Charles Gale and Eivind Osnes, *Phys. Rev.* **C46**, 736 (1992).
23. M. Prakash, T.L. Ainsworth and J.M. Lattimer, *Phys. Rev. Lett.* **61**, 2518 (1988).
24. J. Cugnon, D. L'Hôte and J. Vandermeulen, *NIM* **B111**, 215 (1995).
25. Declan Persram and Charles Gale, **nucl-th/9901019**.
26. E. Conlin et.al., *Phys. Rev.* **C57**, R1032 (1998).
27. R. Sun, private communication.
28. Jianming Zhang, Subal Das Gupta and Charles Gale, *Phys. Rev.* **C50**, 1617 (1994).